Desalination and Water Treatment
www.deswater.com

doi: 10.5004/dwt.2017.21371

89 (2017) 53–64
September

Direct contact and sweeping gas membrane distillation for process intensification – a comparative study

Le My Dinh, Paul Jacob, Chettiyapan Visvanathan*

School of Environment, Resources and Development, Asian Institute of Technology, P.O. Box 4, Klong Luang, Pathumthani 12120, Thailand, emails: visu@ait.asia (C. Visvanathan), dinhlemy90@gmail.com (L.M. Dinh), paul.jacob.env@hotmail.com (P. Jacob)

Received 18 February 2017; Accepted 26 August 2017

ABSTRACT

Sodium sulphate, a salt commonly found in nature and used in industrial applications, was assessed for process intensification from 40 to 450 g/L with two membrane distillation configurations namely direct contact membrane distillation (DCMD) and sweeping gas membrane distillation (SGMD). The polytetrafluoroethylene (PTFE) membrane with 0.45 μm pore size, 50% porosity in hollow fiber (HF) configuration was used in the experimental runs. The optimum conditions, based on pure water tests for both configurations were; feed temperature (70°C both configurations), permeate temperature (ambient air for SGMD, 15°C for DCMD), feed flow rate (2.4 L/min for both configurations) and permeate fluid flow rate (25.5 L/min of ambient air for SGMD, 1.32 L/min with water for DCMD). Despite reaching the saturation concentration of Na_2SO_4, the flux in SGMD and DCMD slightly decreased from 3.1 to 1.9 kg/m^2 h and 1.1 kg/m^2 h, respectively. The average energy consumption of DCMD system at 5.1 kWh/kg was markedly higher as compared with the energy consumption in SGMD system was 1.2 kWh/kg. In addition, at the saturation point, gain output ratio (GOR) for SGMD was three times higher than DCMD which concluded that SGMD system utilized thermal energy more efficiently; noting that SGMD was a favorable configuration in concentrating sodium sulphate solution as compared with DCMD. In terms of resistance analysis, inorganic fouling was overcome after simple cleaning process.

Keywords: Direct contact; Energy consumption; Fouling analysis; Membrane distillation; Permeate flux; Sodium sulphate; Sweeping gas

1. Introduction

Researchers have documented recovery of a variety of minerals using both standalone and coupled membrane-based techniques such as reverse osmosis and membrane distillation (MD) to concentrate and purify salts ranging from ocean water to industrial effluent [1–5]. Sodium sulphate is one such salt which could be a recoverable substance that is present in brine as well as industrial wastewater. This salt is used in a variety of industries such as; filler in laundry detergents, production of wood pulp, glass, textile [6] and phenols. As this compound is used in intermediate processes it ends up in wastewater as total dissolved solids together with other salts. In special cases at high concentrations, removal from industrial wastewater is a challenge. Therefore, some investigators have conducted experiments to separate this valuable compound from wastewater through the combination of various membrane-based technologies including MD and membrane crystallizers [3,5,7] with an intent of environmental sustainability.

MD is a thermally-driven separation process. Unlike other types of filtration method, this process works under the atmospheric pressure. The vapor pressure of a volatile substance is raised by increasing the temperature of feed solution. In contrast, the temperature in the permeate side is generally kept lower than that of feed side to decrease the vapor pressure and collect/condense the generated vapor. The difference in vapor pressures between two sides of membrane, leads to the evaporation of volatile substance at the liquid–vapor interface inside a hydrophobic microporous membrane. Thus, MD can utilize low-grade heat

* Corresponding author.

which creates ideal conditions for exploiting waste heat from industrial processes.

Depending on the application, the end product from MD could be supersaturated salt solution and/or clean water. Since MD can be operated with a high concentration salt solution, normally, temperature polarization could occur that results in crystal formation on the membrane surface. The crystallization process includes nucleation and crystal growth. In the phase of nucleation, dispersed solute molecules gather into clusters. These clusters are required to meet a critical size to move to the crystal growth phase. One of the main factors that dictates the critical size of clusters is temperature. Specifically, in the case of sodium sulphate, the critical cluster size tends to decrease, leading to reduced solubility of the compound when temperatures are higher than 32.38°C [8]. Therefore, the salt crystal would not preferentially form on the membrane surface before they appear in the bulk feed. In this case, temperature polarization had a favorable effect [9] which in turn makes the flux more stable during process intensification to a large extent.

Feasibility of MD to remove salt is undeniable but within MD there are various configurations including direct contact membrane distillation (DCMD), sweeping gas membrane distillation (SGMD), air gap membrane distillation (AGMD) and vacuum membrane distillation (VMD). The fundamental difference between the four configurations are dependent on the way vapor is condensed or recovered on the permeate side. The simplest configuration of MD is direct contact membrane distillation in which, both warm feed and cold permeate aqueous solution are contacted in direct with the hydrophobic membrane. Majority of papers published in this sector are utilizing DCMD configuration [10]. One of the biggest challenge of DCMD systems is that the cool aqueous solution on the permeate side results in a large conductive heat loss through the thin membrane. In the sweeping gas membrane distillation (SGMD) configuration, the vapor at the permeate membrane side is swept out by gas and after that condensed by a separate condenser. The gas is responsible as a barrier not only to reduce the heat loss but also to enhance the mass transfer coefficient [10]. However, SGMD requires a large volume of gas to push out tiny volume of permeate vapor. As most studies on MD are on desalination [11–14], the primary focus has been to recover the permeate and its quality for drinking or other application. However, from a process intensification point of view, where concentrate is of interest rather than the permeate, appropriate configurations need to be considered. To the best of the authors' knowledge, only few researches have studied MD by one more configurations [15,16]. This leads to lack of comparative data between the MD configurations itself for process intensification applications. Thus, a comparative study between MD configurations on its treatment ability, flux, energy consumption (EC) and fouling phenomena is needed. In view of this research gap, such a comparative study using two membrane configurations (SGMD and DCMD) were carried out using sodium sulphate (Na_2SO_4) solution as feed. The performances were compared to assess which of the two configurations would be better suited for a feed with very high amount of sodium sulphate.

2. Transportation in membrane distillation

2.1. Mass transfer

Due to the difference in temperature (difference in vapor pressure) between the feed and permeate side, the vapor can pass through the hydrophobic membrane. Transport mechanism in MD consists of three steps, first, volatile compounds start evaporating in the hot membrane surface; second, vapor is pushed through the hydrophobic membrane by vapor pressure difference and finally, an inert gas in SGMD configuration or water in DCMD configuration carry this vapor out of the membrane module. In all MD configurations, the volume difference of permeate solution at a certain time is used to determine the permeate flux. In theory, the following equations calculate the flux [14]:

$$J_w = B_w \Delta p_w = B_w \left(p^0_{w,f} a_{w,f} - p_{w,p} \right) \tag{1}$$

where B_w, a_w and p_w are the membrane coefficient, activity of water and partial pressure of water, respectively.

The difference in flux calculation between SGMD and DCMD is the partial pressure determination in permeate side.

2.1.1. Mass transfer in DCMD

In DCMD configuration, permeate vapor pressure is calculated similarly with the vapor pressure in feed side:

$$p_{w,p} = p^0_{w,p} \times a_{w,p} = p^0_{w,p} \times \gamma_{w,p} \times x_{w,p} \tag{2}$$

$$\text{With: } p^0_w(T) = \left[\exp\left(23.1964 - \frac{3816.44}{T - 46.13} \right) \right] \tag{3}$$

where x_w, T and γ_w are the water mole fraction, absolute temperature and activity coefficient, respectively.

In the case of feed aqueous solution containing non-volatile compounds, the vapor pressure of the solution is calculated by the following formula:

$$p_{w,s} = (1 - x_s) p_w \tag{4}$$

where x represents the mole fraction of non-volatile solute.

2.1.2. Mass transfer in SGMD

While in SGMD configuration, the permeate partial pressure is expressed as a function of humidity ratio (ω) and the total pressure in the permeate side (P):

$$p_{w,p} = \frac{\omega \times P}{\omega + 0.622} \tag{5}$$

Furthermore, humidity ratio is defined as the relationship between flow rate of sweeping gas ($\dot{m}$), effective membrane area (A), permeate vapor flux (J_w) and the inlet humidity ratio (ω_{in}):

$$\omega = \omega_{in} + \frac{J_w A}{\dot{m}_a} \tag{6}$$

In MD, feed and permeate side are separated by a hydrophobic membrane which allows the volatile component to pass through the membrane layer. Evaporation of volatile compounds at the bulk feed leads to a rise in the concentration of non-volatile compounds at the membrane surface. On the other hand, the volatile compound concentration at the membrane surface is lower than in the bulk feed. However, the concentration of solute components is equal between bulk feed and membrane surface (under turbulent conditions). Therefore, the impact of concentration polarization on flux is negligible [17]. Thus, not considered in this study.

2.2. Heat transfer

Like mass transfer, heat transfer appears at two boundary layers (feed and permeate) and on the membrane. Heat transfer at the boundary layers is discussed in the next section. Heat transfer through the membrane (Q_m) includes conductive heat through membrane material, gas filled inside membrane pores (Q_c) and latent heat accompanying the vapor (Q_v) [14]:

$$Q_m = Q_c + Q_v \tag{7}$$

Following two equations are used to calculate conduction heat and latent heat that are associated with vapor, respectively:

$$Q_c = -k_m \frac{dT}{dx} = \frac{k_m}{\delta}\left(T_{m,f} - T_{m,p}\right) \tag{8}$$

where k_m is the membrane thermal conductivity, δ is the membrane thickness, x is the distance between membrane surfaces. $T_{m,f}$ and $T_{m,p}$, respectively, are temperatures at the feed membrane surface and permeate membrane surface.

$$Q_v = J_w \times \Delta H_{v,w} \tag{9}$$

where J_w and $\Delta H_{v,w}$ are water flux and latent heat of vapor molecule.

2.2.1. Heat transfer at two boundary layers in DCMD configuration

There is a difference in calculation of heat transfer in permeate boundary layer between SGMD and DCMD.

In DCMD configuration, the heat transfer in feed and permeate boundary are indicated by the following equations:

At the feed boundary layer:

$$Q_f = h_f \times \left(T_{b,f} - T_{m,f}\right) \tag{10}$$

At the permeate boundary layer:

$$Q_p = h_p \times \left(T_{m,p} - T_{b,p}\right) \tag{11}$$

where h_f is the coefficient of heat transfer in feed side and h_p is the coefficient of heat transfer in the permeate.

The heat transfer is the same in two boundary layers and membrane module at steady-state condition:

$$Q_f = Q_p = Q_m \tag{12}$$

$$h_f\left(T_{b,f} - T_{m,f}\right) = h_p\left(T_{m,p} - T_{b,p}\right) = \frac{k_m}{\delta}\left(T_{m,f} - T_{m,p}\right) + J_w \Delta H_{v,w} = H\left(T_{b,f} - T_{b,p}\right) \tag{13}$$

where H refers to the coefficient of global heat transfer and $\Delta H_{v,w}$ is latent heat of water evaporation.

The temperature at surface of membrane cannot be measured directly. Thus, using empirical correlations it can be calculated using heat transfer coefficient [16]:

$$h = \frac{Nuk}{d_h} \tag{14}$$

where k and d_h are fluid thermal conductivity and hydraulic diameter, respectively.

Nusselt number (Nu) is defined as the ratio between convective and conductive heat transfer through boundary layers that is calculated by Eq. (15):

$$Nu = 1.86 \times \left(\mathrm{Re} \times \mathrm{Pr} \times \frac{d_h}{L}\right)^{1/3} \tag{15}$$

Pr is Prandtl number that is evaluated by the following formula:

$$\mathrm{Pr} = \frac{\mu C_p}{k} \tag{16}$$

where Re, L, μ, C_p and k are Reynolds number, effective length of membrane, dynamic viscosity, specific heat and thermal conductivity, respectively.

The temperature at surface of membrane can be determined by Eqs. (17) and (18):

$$T_{m,f} = \frac{\frac{k_m}{\delta}\left(T_{b,p} + \frac{h_f}{h_p}T_{b,f}\right) + h_f T_{b,f} - J_w \Delta H_{v,w}}{\frac{k_m}{\delta} + h_f\left(1 + \frac{k_m}{\delta h_p}\right)} \tag{17}$$

$$T_{m,p} = \frac{\frac{k_m}{\delta}\left(T_{b,p} + \frac{h_p}{h_f}T_{b,p}\right) + h_p T_{b,p} - J_w \Delta H_{v,w}}{\frac{k_m}{\delta} + h_p\left(1 + \frac{k_m}{\delta h_f}\right)} \tag{18}$$

2.2.2. Heat transfer at two boundary layers in SGMD configuration

In SGMD configuration, the heat transfer through feed boundary layer and permeate boundary layer can be expressed as following equations:

$$Q_f = h_f \times \left(T_{b,f} - T_{m,f}\right) \tag{19}$$

$$Q_a = h_a \times \left(T_{m,p} - T_{b,p}\right) \tag{20}$$

where h_f and h_a are heat transfer coefficients of feeding solution and sweeping gas, respectively.

h_f can be calculated by Eqs. (14)–(16).

h_a can be calculated by the following equation [18]:

$$h_a = 0.206\left(\frac{k}{d_h}\right)\left(Re.\cos\alpha\right)^{0.63}\mathrm{Pr}^{0.36} \tag{21}$$

where yaw angle α is 0 for cross flow and for the parallel flow, this value is 90.

In stable condition, the heat transfer through permeate boundary layer can be represented by the following formula:

$$Q_a = \frac{\dot{m}_a\left(c_a + \omega_{\mathrm{in}} c_w\right)\left(T_{a,\mathrm{out}} - T_{a,\mathrm{in}}\right)}{A} + J_w\left(\Delta H_v^0 + c_w T_{a,\mathrm{out}}\right) \tag{22}$$

where $\dot{m}_a$, c_a, c_w, ω, $T_{a,\mathrm{out}}$ and $T_{a,\mathrm{in}}$ are gas flow rate, specific heat of air, specific heat of water, humidity ratio, air temperature out and in, respectively.

2.2.3. Temperature polarization coefficient

The heat transfer also appears on boundary layers. The high viscosity of feed solution and low flow rate resulted in the difference of temperature in the bulk and membrane surface which is called temperature polarization. These boundary layers impose the resistance to heat transfer leading to reduced membrane flux. Temperature polarization coefficient (TPC) used to measure the impact of temperature polarization on the driving force. TPC can be expressed as:

$$\mathrm{TPC} = \frac{T_{m,f} - T_{m,p}}{T_{b,f} - T_{b,p}} \tag{23}$$

The subscripts *m*, *f*, *p* and *b* are membrane, feed, permeate and bulk, respectively.

3. Materials and methods

3.1. Membrane characteristics

The polytetrafluoroethylene (PTFE) hydrophobic microporous hollow fiber (HF) membrane with a contact angle of 112°, nominal pore size 0.45 μm, 50% porosity, thickness of 480 μm and an estimated liquid entry pressure of 119.9 kPa was used in this study. Sumitomo Electric Company Ltd. (Osaka, Japan) manufactured this module. The membrane module had a packing density at 333.8 m^2/m^3. The effective membrane area was 0.255 m^2.

3.2. Feed characteristics

Sodium sulphate (Na_2SO_4, CAS No.7757-82-6, Alpha Chemika, Maharashtra, India) and deionized water (18.2 MΩ cm^{-1}) were used for feed preparation. The experiments were conducted with an initial feed concentration of 40 g/L sodium sulphate in both configurations. The concentration of sodium sulphate in the solution estimated using procedure 2540 C [19].

3.3. Experimental setup

The laboratory scale schematic combined DCMD and SGMD are presented in Fig. 1. As the difference between sweeping gas and DCMD is the carrier fluid (liquid/gas), the setup was modified as per experimental protocol. The membrane module was operated in outside in configuration. Temperature probes and pressure probes were located on the inlet and exit of the feed pipe to the membrane module and were monitored for operational purposes. In this setup, the feed tank (10 L working capacity) was accompanied with a heater controlled by a thermal sensor. The feed tank could be heated to a range of 30°C–100°C. As it was a closed system, the level indicator on the feed tank was used to observe/calculate the flux. On the feed tank, insulation layer was provided to minimize the heat loss to the environment. In DCMD, the permeate was deionized water, which was in contact with a chiller via a heat exchanger to maintain 15°C. In SGMD, ambient air was used as a carrier fluid. Laboratory air compressor was used to supply the sweeping gas; a gas flow meter measured the air flow rate. An external condenser was not installed in SGMD system to minimize the process complexity. Moreover, in process intensification process, permeate collection is not a necessary concern. Energy loggers were integrated to determine the EC of the processes.

As the operation for both configurations were opted to be semi-continuous to determine the maximum obtainable flux. Divalent salt solution was added into the feed tank after every 8 h with the concentration of the next batch 10% lower than the end concentration of previous batch. In addition, the volume of the feed solution was maintained at 10 L while starting a new batch. The membrane module was rinsed with water during this time to prevent crystal formation causing damage to the membrane.

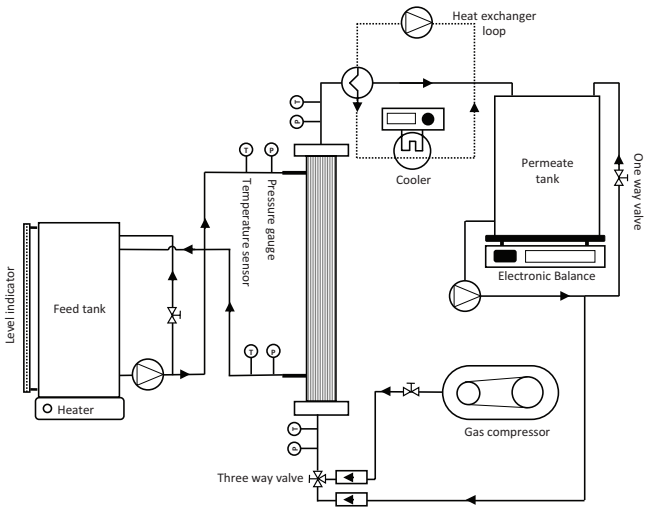

Fig. 1. Experiment setup of lab-scale hollow fiber membrane distillation.

3.4. Pure water flux and salt rejection

Pure water flux measurement was done using deionized (DI) water in SGMD and DCMD configuration. In the case of SGMD, the feed flow rate was kept at 2.4 L/min, while the temperature was varied between 50°C and 70°C with gas flow rates of 16.9, 19.6, 22.5, 25.5 and 28.5 L/min. After the highest permeate flux was found for SGMD, the same feed temperature was used for DCMD with varying permeate flow rate. The permeate flow rates were varied (0.74, 1.06, 1.32, 1.69, 2.1, 2.51 and 2.68 L/min). The permeate flux (kg/m^2 h) was calculated by dividing the total mass loss rate (kg/h) by effective membrane area (m^2). The mass of water lost in the heater was exactly the amount of permeate passed through the membrane which was calculated by multiplying the volume of water loss by specific density of water. The calculation of flux (kg/m^2 h) is expressed as Eq. (24):

$$J_w = \frac{\left(V_1 - V_2\right) \times \rho_w}{A \times t} \tag{24}$$

where V_1 (L) is the volume of feed solution, V_2 (L) is the measured volume after 1 h, A (m^2) is membrane surface area, ρ_w (kg/L) is specific density of water, t (h) is duration, in this case, t equal to 1 h.

The rejection test was performed using 1% saline solution. The test was done to ensure only volatile compound (water) passed through the hydrophobic membrane and non-volatile compound (salt) retained in the feed solution. The percentage of rejection (R%) was calculated by using following Eq. (25):

$$R(\%) = \left(\frac{C_f - C_p}{C_f}\right) \times 100 \tag{25}$$

where C_p (ppm) is permeate concentration and C_f (ppm) is feeding concentration.

3.5. Membrane cleaning and fouling analysis

Membrane after a certain time becomes fouled thus reducing the membrane flux. Therefore, membrane cleaning was done to remove fouling on the membrane surface at the end of the operation. Rinsing membrane module with DI water was implemented as a recoverable method (before feeding every batch) and it was also used to remove remaining chemical after cleaning the membrane. Inorganic fouling (sodium sulphate/sodium chloride) was washed out by dilute acidic solution (0.1 wt% oxalic acid and 0.8 wt% citric acid) for 6 h. As the feed is a binary solution of water and salt, the authors assumed no organic fouling to occur on the membrane surface, thus did not treat it using base solution; nor account it for overall resistance calculations.

The overall resistance (R_t) includes membrane resistance (R_m), boundary layer resistance (R_b) and fouling resistance (R_f). Membrane resistance was estimated by using DI. Fouling resistance consisted of recoverable fouling resistance (R_r) that was evaluated after washing membrane with DI water, reversible fouling (R_{re}) and irreversible fouling (R_{ir}) were identified by cleaning membrane with chemicals. The overall resistance was calculated as follow [20]:

$$R_t = R_m + R_f + R_b = R_m + R_r + ir + R_{re} + R_b \tag{26}$$

In which each type of resistance was calculated as per equations below:

Total fouling resistance (R_t)

$$R_t(\text{m/s}) = \frac{P_f - P_p}{J_w} \tag{27}$$

where P_f and P_p are vapor pressure at feed and permeate side, respectively.

Feed boundary layer resistance ($R_{b,f}$)

$$R_{b,f}(\text{m/s}) = \frac{P_{b,f} - P_{m,f}}{J_w} \tag{28}$$

where $P_{b,f}$ and $P_{m,f}$ are vapor pressures at bulk feed and membrane feed, respectively.

Permeate boundary layer resistance ($R_{b,p}$):

$$R_{b,p}\left(\text{m/s}\right) = \frac{P_{b,p} - P_{m,p}}{J_w} \tag{29}$$

where $P_{b,p}$ and $P_{m,p}$ are bulk permeate and membrane permeate vapor pressures, respectively.

Boundary layer resistance (R_b):

$$R_b(\text{m/s}) = R_{b,f} + R_{b,p} \tag{30}$$

Fouling resistance (R_f):

$$R_f(\text{m/s}) = R_t - \left(R_b + R_m\right) \tag{31}$$

Recoverable fouling (R_r): R_{f1} was calculated using the flux after rinsing with DI water for 30 min.

$$R_r(\text{m/s}) = R_f - R_{f1} \tag{32}$$

Reversible fouling (R_{re}): R_{f2} used the flux of the system after cleaning with acidic solution and DI water:

$$R_{re}\left(\text{m/s}\right) = R_{f1} - R_{f2} \tag{33}$$

Irreversible fouling (R_{ir}):

$$R_{ir} = R_f - \left(R_r + R_{re}\right) \tag{34}$$

3.6. Energy consumption

An energy meter was installed on the system to measure the amount of energy consumed by the whole system. The energy observed included energy consumed for heating or/and cooling as well as energy used for pumping. Finally, the EC (kWh/kg), where kWh of energy required to produce a unit of permeate (kg), can be calculated by dividing the total observed energy (kWh) by the flux (kg/m^2 h) and membrane area (m^2) as given in Eq. (35).

$$EC = \frac{\text{Observed energy}}{J_w \times A} \quad (35)$$

Moreover, the energy comparison between DCMD and SGMD was more equitable by calculating gained output ratio (GOR), in which only thermal energy was put into concern. GOR is the ratio between latent heat and total heat input to maintain the temperature of the feeding solution that indicates the thermal efficiency of MD system:

$$GOR = \frac{Q_v \times A}{F_f \times \rho_f \times C_p \times (T_{f,\text{in}} - T_{f,\text{out}})} \quad (36)$$

where F_f (L/h) is the feed solution circulation rate, $T_{f,\text{in}}$ and $T_{f,\text{out}}$ are temperatures of feeding solution before and after passing through membrane module.

4. Result and discussion

4.1. Salt rejection, pure water flux and energy consumption

4.1.1. Pure water flux

In MD, the temperature of feed with permeate fluid flow rate has a high influence on the flux. The increase of feed temperature from 50°C to 60°C enhanced the membrane flux by 74%. The highest flux falls into the group with feed temperature of 70°C with more than 199% higher flux value compared with the flux at 50°C. Accompanying the feed temperature, the gas flow rate was detected as the dependent operating parameter that used to control the flux membrane.

As presented in Table 1, it can be noted that at the same feed temperature an increase in sweeping gas flow rate resulted in an increase in membrane flux. The gas flow rate enhancement promoted the heat transfer coefficient on the permeate side. Therefore, the effect of temperature polarization was reduced. However, its effect on membrane flux was not significant as in the case of feed temperature. For example, at the same feed temperature of 60°C, the membrane flux increased by only 40% when increasing the sweeping gas flow rate from 16.9 to 28.5 L/min. Khayet and Matsuura [10] also concluded that the feed inlet temperature affects more significantly than a higher gas circulation velocity. When the gas flow rate was increased from 25.5 to 28.5 L/min, it should be noted that the flux reduced by 14%, this may be due to additional resistance caused by pressure generated by the high gas flow rate. A similar reduction in the membrane flux was also observed with further increase in sweeping gas flow rate [21]. As established previously (flux wise), 70°C for SGMD was better. Thus, the same temperature was used to study the effect of permeate flow rate on the flux in DCMD setup, where feed flow rate

Table 1
Pure water flux with different operating conditions in this study and literature

Configuration	Feed	ΔT (°C)	Permeate fluid flow rate (L/min)	Flux (kg/m² h)	Energy consumption (kWh/kg)	Reference
HF SGMD	Water	(50 – 30)	16.9	0.52	2.70	This study
		20	19.6	0.78	2.00	
			22.5	1.05	1.58	
			25.5	1.05	1.71	
			28.5	1.05	2.14	
		(60 – 30)	16.9	1.31	1.39	
		30	19.6	1.57	1.27	
			22.5	1.83	1.34	
			25.5	1.83	1.43	
			28.5	1.57	1.64	
		(70 – 30)	16.9	1.83	1.35	
		40	19.6	2.09	1.31	
			22.5	2.61	1.07	
			25.5	3.14	1.09	
			28.5	2.70	1.32	
HF DCMD		(70 – 15)	0.74	2.61	3.86	
		55	1.06	2.61	3.93	
			1.32	2.88	3.63	
			1.69	2.88	3.68	
			2.1	2.88	3.64	
			2.51	2.88	3.73	
			2.68	2.88	3.77	
HF AGMD	NaCl 3.5%w	55	–	12.5	–	[23]
HF DCMD	NaCl 9.09%	45	–	16.5	–	[24]
HF VMD	NaCl 9.09%	45	–	23.5	–	[24]

and feed/permeate temperature were kept constant. It was found that at permeate flow rate of 1.32 L/min, the flux was 2.88 kg/m² h and after that even with the additional increase in flow rate, no increase in flux was observed. It is noticeable that at the optimum condition found in this study, the SGMD flux was slightly higher than DCMD flux which was also observed in the literature [22]. It can also be noted for both MD configuration in this study, the flux compared with other studies is lower, and this is due to the low porosity (50%) and high thickness (about four times than flat sheet membranes in literature). However, the HF membrane used in this study had a high packing density which means filtration area per volume of the membrane is high. Thus from a commercial point of view, HF is more attractive than flat sheet membrane.

4.1.2. Salt rejection

The rejection tests for SGMD configuration were conducted with a gas flow rate of 16.6 L/min (lowest) and 28.5 L/min (highest) at a feed temperature of 70°C for 4 h each. It was found with an average flux of 1.83 and 2.88 kg/m²h and a rejection of 99.99% the membranes used for the study could work with the MD principles in SGMD configuration. As the membranes were performing well under SGMD configuration the authors also assumed the same for DCMD configuration.

4.1.3. Energy analysis

As one of the principal advantages of MD is its ability to extract water below its boiling point. Within the two-studied configurations, additional to pure water flux, EC was studied and it was found that at feed temperature of 70°C, permeate fluid flow rate 25.5 (for SGMD) and 1.32 (DCMD) L/min, the EC was 1.09 and 3.63 kWh/kg, respectively. SGMD had a lower EC as the permeate inherently was not condensed for the process to work, unlike DCMD configuration. Moreover, DCMD had a lower thermal efficiency than SGMD which was expressed through the GOR value. The SGMD configuration reached a GOR value of 3.6 that was two times higher the GOR from DCMD system at 1.8. A study in AGMD shows the GOR value in the range of 6–9.5 which is much higher than this study because their distillate production rate was high at 4–10 L/h [25]. However, specific MD configuration would have more advantages compared with conventional processes. Table 2 presented the EC comparison between MD and other conventional process used for desalination. MD uses the less energy among those desalination processes because MD can work under the boiling point of water or atmospheric pressure.

To summarize from observations made with pure water flux, salt rejection and EC, the optimum temperature for both configuration was 70°C, permeate fluid flow rate 25.5 (for SGMD) and 1.32 (DCMD) L/min, when feed flow kept at 2.4 L/min, temperature of permeate was ambient temperature of 27°C ± 3°C for SGMD and 15°C for DCMD.

4.2. Sodium sulphate removal using SGMD

The total experimental duration to concentrate from 40 to 450 g/L took 30 h. As presented in Fig. 2, the permeate flux did not significantly change when the salt concentration increased. The flux decreased slightly from 3.07 to 1.95 kg/m² h when the salt concentration increased from 40 g/L to around 450 g/L. The salt solution had a low viscosity, therefore, the effect of the boundary layer and its related resistances were minimal. Temperature polarization phenomena suggest that the temperature was lower on the membrane surface than observed in the bulk side of the membrane [18]. In addition, solubility of the salt has a close relationship with temperature. Depending on the type of salt (positive solubility or negative solubility), the solubility is proportional or inversely proportional to the temperature. Sodium sulphate has negative solubility, implying higher solubility at lower temperature. This trend was predicted by using Le Chatelier's principle. Sodium sulphate dissolved in water as an exothermic reaction. Per the equilibrium law, external heat caused the equilibrium to the exothermic process by moving towards the reactants. Therefore, the salt crystal did not form on the membrane surface before it appeared in the bulk feed. The concentration reached around 450 g/L then some salt crystals started to form and accumulate on the membrane surface. As seen in Fig. 2, the concentration of feed solution reached supersaturation, membrane flux declined because of the rapid formation of salt crystal on the surface of membrane. TPC value in SGMD increased from 0.1 to 0.3 with an increase of feed concentration, similar observation are found using DCMD [26]. Khayet and Matsuura [10] also observed SGMD system (plate and frame configuration) gave a TPC of less than 0.44. Solute accumulation on feed membrane surface leading to increase in boundary layer thickness can be attributed to the increase in TPC as the feed concentration increases.

The result from Fig. 2 also indicated that at low salt concentration (40–285 g/L), the EC was ~1.07 kWh/kg. However, the required EC tends to increase when solution reached supersaturation. As above 285 g/L of sodium sulphate, EC increased up to 1.37 kWh/kg. This was due to the decline in flux while the energy demand from the system was constant. In air gap MD configuration, the ratio of consumed energy and water production was about 12 kWh/kg where the feed was 10.6 g/L of Na_2SO_4 at 50°C of feeding temperature [27]. The GOR decreased from 3.4 to 1.6 which means the heat loss was higher as the feeding solution got denser.

Table 2
Comparison between MD and conventional method in desalination process

Process	Energy consumption (kWh/kg)	Reference
Air gap membrane distillation	1.85	[14]
Reverse osmosis	1.37	
Multi-stage flash distillation	5.63	
Multi-effect distillation	4	
Multi-effect solar still	25	
HF SGMD	1.09	This study
HF DCMD	3.63	This study

4.3. Sodium sulphate removal using DCMD

Similar to SGMD, when the setup was operated in DCMD configuration the feed could be concentrated from 40 g/L to around 450 g/L in 52 h. Alternatively, Li et al. [7] coupled a reverse osmosis (RO) system with a membrane crystallization, where RO was used to concentrate Na_2SO_4 solution to 150 g/L, and after that membrane crystallization was used. As can be seen from Fig. 3, initially, the flux slightly decreased from 3.07 to 2.51 kg/m^2 h, while with the salt concentration was higher than 200 g/L and came closer with saturation point, the flux was reduced more significantly from 2.51 to 1.12 kg/m^2 h. When the concentration of Na_2SO_4 solution was ~450 g/L, the salt crystals were observed on the membrane surface. In the investigated range, the results of the experiment showed a decline of membrane flux of 63.5%. Nghiem et al. [28] studying DCMD system also observed a sudden drop of permeate flux with calcium sulphate solution at saturation point. In DCMD configuration, the boundary layers are recognized as a factor that limits the flux. The TPC was higher from 0.74 to 0.76 with increasing concentration of salt solution.

The heater and cooler equipment represented as the main consumed energy sources of the DCMD process. As presented in Fig. 3, the energy required for DCMD remained stable at low concentration with the average value of ~3.6 kWh/kg. Criscuoli et al. [29] presented while using DCMD configuration the lowest energy required for their system was 3.55 kWh/kg, where feed temperature varied from 40°C to 60°C while permeate temperature was changed from 13°C to 14°C. However, the required energy rose to 60% of energy demand compared with working with the initial concentration of 8.44 kWh/kg. The reason for this extreme change of EC was the flux reduction at high salt concentration. In addition, the significant decrease of GOR from 1.7 to 0.5 provided evidence that feeding concentration had a negative effect to the thermal efficiency of the system.

4.4. Fouling analysis in SGMD configuration

The fouling analysis was similar between DCMD and SGMD configuration because the salt concentration and contact time did not effect on the fouling of negative solubility salt. Thus, the study focuses on fouling analysis in SGMD configuration. MD process is generally affected by membrane resistance and boundary layer resistance. The membrane resistance that was evaluated by the pure water test is constant, and boundary resistance closely depends on the concentration of feed solution. However, the analysis revealed that as the salt concentration increased from 40 to 450 g/L,

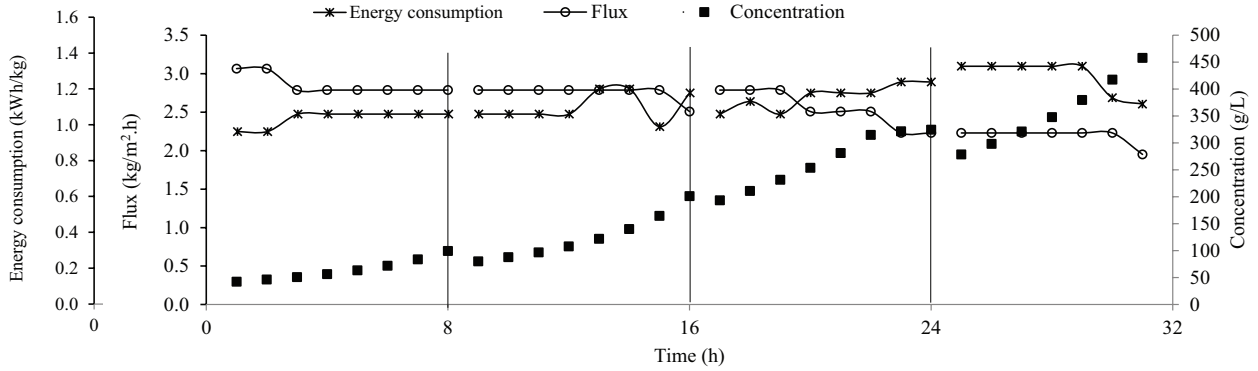

Fig. 2. Performance of HF SGMD in the operation with high concentration Na_2SO_4 solution.

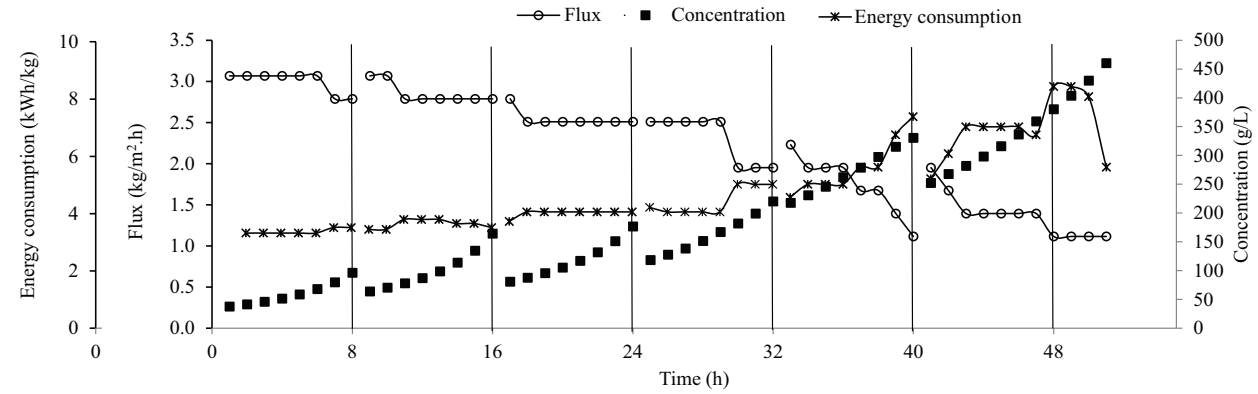

Fig. 3. Performance of HF DCMD in the operation with high concentration Na_2SO_4 solution.

the contribution of boundary layer resistance increased insignificantly from 27.5% to 33.2%, while membrane resistance was still the highest form of resistance. Therefore, the sodium sulphate concentration had a minor effect on the boundary layer resistance. No flux reduction or wetting of membrane surface was observed during reclamation process of Na_2SO_4 from industrial wastewater utilizing MD [3]. Similarly, no wetting was observed in the current study.

Fouling analysis in MD with the highest concentration of the salt solution was conducted to consider the portion of different types of resistance. The inorganic fouling was generated due to the formation of sodium sulphate crystallization. The crystal nucleation appeared at supersaturation condition. The different resistances contributions are grouped in Fig. 4. The highest resistance accounted for 44.7% that was localized in membrane resistance while the inorganic fouling at 33.2% was lower than membrane resistance but higher than boundary layer resistance at 22.1 %. The negative solubility of sodium sulphate salt is a rational reason to explain this phenomenon. A negative soluble salt is more solvable at low temperature than at high temperatures; implying that the crystal did not preferentially form on the membrane surface. Additionally, rinsing membrane with DI water every 8 h is also the reason of the negligible influence of inorganic fouling. The membrane was recovered by running with DI water for around 30 min with recoverable fouling accounted for 25.5%. In addition, MD was further cleaned by citric and oxalic solution that resulted in 7.7% of reversible fouling.

4.5. Comparison between SGMD and DCMD

At the same condition, initially, the flux for HF DCMD and HF SGMD was relatively equal to 3.07 kg/m^2 h as presented in Fig. 5. The temperature difference between two sides in DCMD configuration (55°C) was greater than in the SGMD (37°C). However, for SGMD configuration, gas temperature contributed slightly to the membrane flux. Ambient temperature (varying between 25°C and 35°C) was observed to be sufficient to utilizing as gas temperature [10]. SGMD was insensitive with the temperature of the permeate gas [21].

The flux in SGMD system seemed to be stable at the initial concentrations and came down to 2 kg/m^2 h at the saturation point, while DCMD flux reduced more significantly and reached 1.12 kg/m^2 h at the end of the experiment. In general, as the salt concentration increased, the DCMD flux decreased more sharply than the flux in SGMD system. At 450 g/L of salt solution, in SGMD configuration, heat transfer coefficients (HTC) of feed side and permeate side were calculated to be 530.9 and 163.6 W/(m^2 K), respectively. Those values were found to be 530.9 and 1,758.1 W/(m^2 K) in DCMD configuration with the same concentration of salt. Permeate side of the DCMD had a higher HTC than that of feed side due to Eq. (14), the smaller hydraulic diameter in permeate side leads to the higher in HTC value. In contrast, higher HTC value of feed side was found as compared with permeate side of the SGMD configuration because water had a considerably greater HTC than that of gas. Therefore, heat transfer was found to occur at the feed side of SGMD and the permeate side of DCMD. The above explanation presents the strong effect of high concentration of feed side on reducing the membrane flux within the DCMD configuration. In addition, the GOR analysis reveals that at saturation concentration of feeding solution, the GOR of SGMD was 1.5 which was three times the GOR from DCMD configuration at 0.5. Thus, SGMD utilized thermal energy more productive than DCMD.

Fig. 6 presents the EC in HF DCMD system which was markedly higher as compared with EC in HF SGMD system. It was since energy used for cooling water in DCMD system was much higher than the energy utilized for supplying gas in SGMD system. Moreover, the internal heat loss through membrane in DCMD promoted more energy (in terms of heat conduction) and resulted in re-heating and re-cooling the feed and permeate solution, respectively. The general performance of DCMD and SGMD configuration in this study is compared with another research as described in Table 3. In addition to DCMD and SGMD, AGMD was also indicated as potential configuration in intensification process. Synthetic brine with the initial concentration of 65 g/L NaCl could be concentrated above the saturation point by using flat sheet AGMD [30].

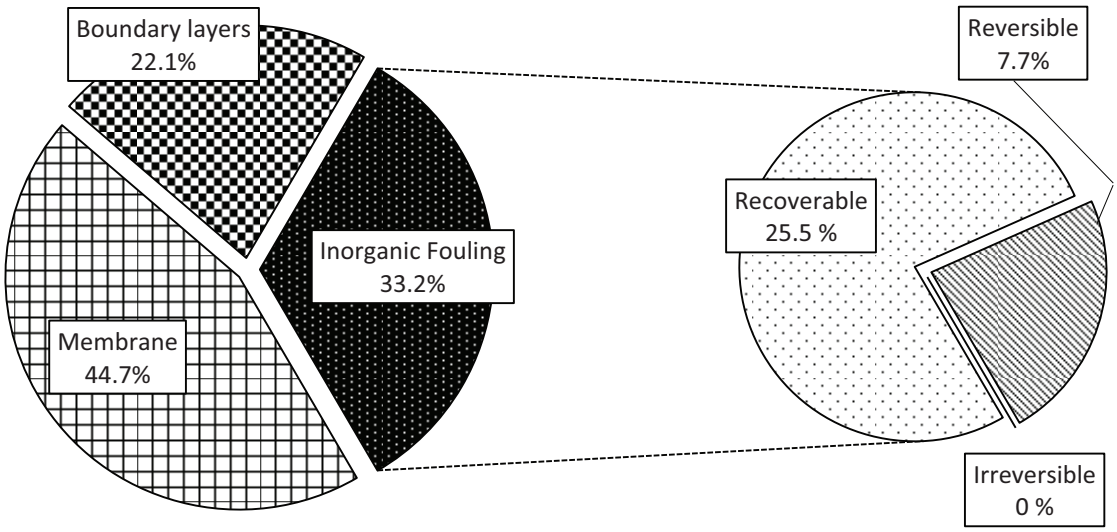

Fig. 4. Different type of resistances in MD with high salt concentration.

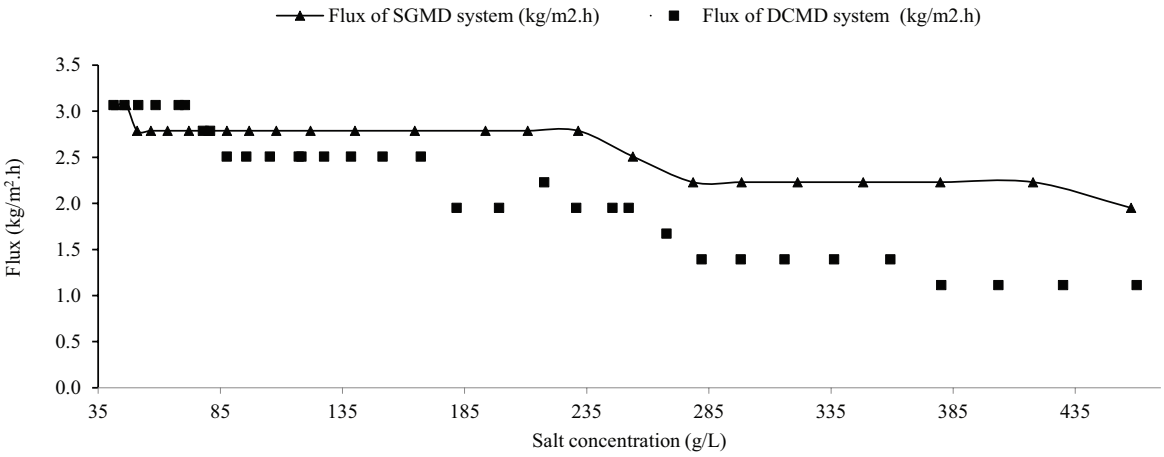

Fig. 5. Flux comparison between SGMD and DCMD.

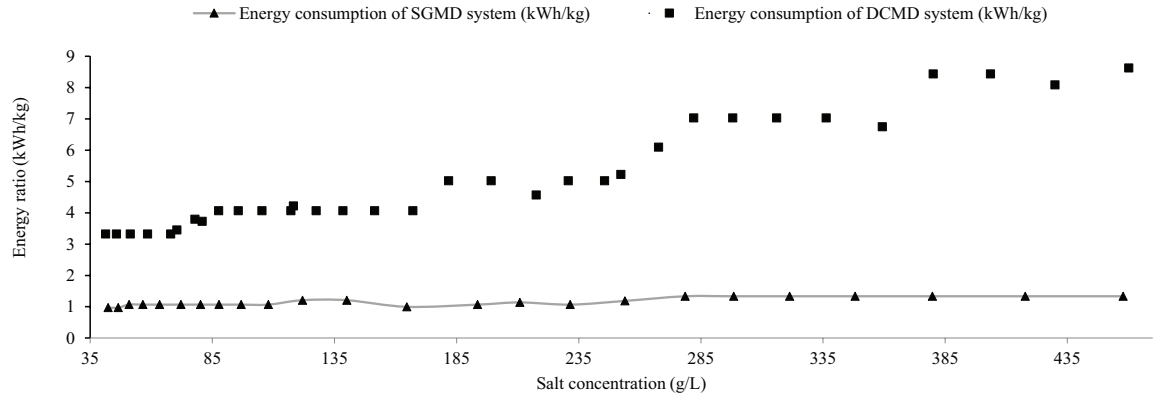

Fig. 6. Energy consumption comparison between SGMD and DCMD.

The study reached highest flux up to 46.50 ± 0.21 kg/m^2 h because of the high different inlet temperatures 82°C. Another study also confirmed that DCMD was able to treat high salt solution which was collected from the North Arm of the Great Salt Lake [31]. The hypersaline brine contains not only sparingly soluble salts but also natural organic matter. The flux reached 25.3 L/m^2 h with a temperature difference of 40°C. The membrane was prevented from fouling damage by limiting the extent of concentration. It is more unfavorable to handle with positive solubility salt. Fouling resistant is problem of MD when dealing with saline brine which contains mostly positively soluble salt solution. In addition, another method to overcome fouling is adding anti-scalant with appropriate dose in the test with seawater by AGMD [32]. However, the EC analyses were not mentioned in these studies.

5. Conclusions

In this work, the Na_2SO_4 solution was treated by DCMD and SGMD configuration using HF PTFE membrane. Their performances were investigated and compared. The following conclusions can be made:

The optimum operating condition of the system using pure water with the gas flow rate of 25.5 L/min in SGMD and the permeate water flow rate of 1.32 L/min in DCMD. The feed temperature was better at 70°C.

In SGMD, the permeate flux was relatively stable at around 2.51 kg/m^2 h when the salt concentration increased from 40 to 450 g/L. In addition, the temperature polarization was observed as a favorable factor for membrane flux at high concentration. The energy consumed in this experiment was 1.07 kWh/kg.

Experiment on DCMD configuration was also successful when operated with a high concentration of Na_2SO_4 solution. The membrane flux decreased from 3.07 to 1.12 kg/m^2 h when salt concentration increased from 40 to 450 g/L. The EC rose from 3.32 to 8.44 kWh/kg at higher salt concentration.

Fouling resistance did not play an important role as the feed was sodium sulphate salt solution. The highest resistance accounted for 45% that was localized in membrane resistance, followed by 33.2% of inorganic fouling resistance and 22.1% of boundary layer resistance. If this compound needs to be concentrated from industrial effluent, other contaminants might cause more fouling and need to be studied depending on the industry.

There was no significant difference in average flux between DCMD and SGMD configuration at 2.2 and 2.6 kg/m^2 h, respectively. However, the EC of DCMD system (5.1 kWh/kg) was markedly higher compared with EC in SGMD system

Table 3
Performance of MD in various studies

Configuration	Feed solution	Temperature (°C)		Maximum reached concentration (g/L)	Energy consumption (kWh/kg)	Fouling phenomena	Reference
		Feed side	Permeate side				
DCMD	Industrial wastewater (40 – 132 g/L Na_2SO_4)	40 ± 10	30 ± 10	370.3	–	No pore blocking after cleaning with citric acid solution and distillate water	[3]
DCMD	Synthetic Na_2SO_4 solution (40 g/L)	65 ± 5	15 ± 3	~450	3.3 – 8.4	Fouling resistance overcame after cleaning with citric and oxalic solution and rinsing with distillate water	This study
SGMD		65 ± 5	29 ± 3		1 – 1.3		

(1.2 kWh/kg) and GOR of SGMD was three times the value from DCMD. Thus, SGMD becomes a better configuration in dealing with high concentration of Na_2SO_4 solution.

Polymer degradation have been observed at very high salt concentrations [33], thus long-term studies are needed before employing technology at industrial scale.

References

[1] A. Ali, C.A. Quist-Jensen, F. Macedonio, E. Drioli, Application of membrane crystallization for minerals' recovery from produced water, Membranes, 5 (2015) 772–792.
[2] K.L. Hickenbottom, T.Y. Cath, Sustainable operation of membrane distillation for enhancement of mineral recovery from hypersaline solutions, J. Membr. Sci., 454 (2014) 426–435.
[3] C.A. Quist-Jensen, F. Macedonio, D. Horbez, E. Drioli, Reclamation of sodium sulfate from industrial wastewater by using membrane distillation and membrane crystallization, Desalination, 401 (2016) 112–119.
[4] K. Ranganathan, K. Karunagaran, D. Sharma, Recycling of wastewaters of textile dyeing industries using advanced treatment technology and cost analysis—case studies, Resour. Conserv. Recycl., 50 (2007) 306–318.
[5] C.M. Tun, A.M. Groth, Sustainable integrated membrane contactor process for water reclamation, sodium sulfate salt and energy recovery from industrial effluent, Desalination, 283 (2011) 187–192.
[6] R.C. Wells, Sodium Sulphate: Its Sources and Uses, US Government Printing Office, Washington, USA, 1923.
[7] W. Li, B. Van der Bruggen, P. Luis, Integration of reverse osmosis and membrane crystallization for sodium sulphate recovery, Chem. Eng. Process. Process Intensif., 85 (2014) 57–68.
[8] P. Bharmoria, P.S. Gehlot, H. Gupta, A. Kumar, Temperature-dependent solubility transition of Na_2SO_4 in water and the effect of NaCl therein: solution structures and salt water dynamics, J. Phys. Chem. B, 118 (2014) 12734–12742.
[9] A. Kurdian, M. Bahreini, G. Montazeri, S. Sadeghi, Modeling of direct contact membrane distillation process: flux prediction of sodium sulfate and sodium chloride solutions, Desalination, 323 (2013) 75–82.
[10] M. Khayet, T. Matsuura, Membrane distillation: principles and applications, Elsevier, Amsterdam, Netherlands, 2011.
[11] A.M. Alklaibi, N. Lior, Membrane-distillation desalination: status and potential, Desalination, 171 (2005) 111–131.
[12] J.-P. Mericq, S. Laborie, C. Cabassud, Vacuum membrane distillation for an integrated seawater desalination process, Desal. Wat. Treat., 9 (2009) 287–296.
[13] D. Wirth, C. Cabassud, Water desalination using membrane distillation: comparison between inside/out and outside/in permeation, Desalination, 147 (2002) 139–145.
[14] S. Yarlagadda, L.M. Camacho, V.G. Gude, Z. Wei, S. Deng, Membrane distillation for desalination and other separations, Recent Pat. Chem. Eng., 2 (2009) 128–158.
[15] C. Huayan, W. Chunrui, J. Yue, W. Xuan, L. Xiaolong, Comparison of three membrane distillation configurations and seawater desalination by vacuum membrane distillation, Desal. Wat. Treat., 28 (2011) 321–327.
[16] S. Cerneaux, I. Strużyńska, W.M. Kujawski, M. Persin, A. Larbot, Comparison of various membrane distillation methods for desalination using hydrophobic ceramic membranes, J. Membr. Sci., 337 (2009) 55–60.
[17] A. Ali, F. Macedonio, E. Drioli, S. Aljlil, O.A. Alharbi, Experimental and theoretical evaluation of temperature polarization phenomenon in direct contact membrane distillation, 60th Anniversary European Federation of Chemical Engineering, Chem. Eng. Res. Des., 91 (2013) 1966–1977.
[18] M. Khayet, M.P. Godino, J.I. Mengual, Theoretical and experimental studies on desalination using the sweeping gas membrane distillation method, Desalination, 157 (2003) 297–305.
[19] APHA, Standard Methods for Examination of the Water and Wastewater, APHA, Washington, D.C., 2005.
[20] S. Srisurichan, R. Jiraratananon, A. Fane, Mass transfer mechanisms and transport resistances in direct contact membrane distillation process, J. Membr. Sci., 277 (2006) 186–194.
[21] L. Basini, G. D'Angelo, M. Gobbi, G. Sarti, C. Gostoli, A desalination process through sweeping gas membrane distillation, Desalination, 64 (1987) 245–257.
[22] M. Khayet, J.I. Mengual, P.P. Godino, Possibility of nuclear desalination through various membrane distillation configurations: a comparative study, Int. J. Nucl. Desal., 1 (2003) 30–46.

[23] R. Aryapratama, H. Koo, S. Jeong, S. Lee, Performance evaluation of hollow fiber air gap membrane distillation module with multiple cooling channels, Desalination, 385 (2016) 58–68.
[24] Y. Tang, N. Li, A. Liu, S. Ding, C. Yi, H. Liu, Effect of spinning conditions on the structure and performance of hydrophobic PVDF hollow fiber membranes for membrane distillation, Desalination, 287 (2012) 326–339.
[25] H.C. Duong, P. Cooper, B. Nelemans, T.Y. Cath, L.D. Nghiem, Evaluating energy consumption of air gap membrane distillation for seawater desalination at pilot scale level, Sep. Purif. Technol., 166 (2016) 55–62.
[26] R. Bouchrit, A. Boubakri, A. Hafiane, S.A.-T. Bouguecha, Direct contact membrane distillation: capability to treat hyper-saline solution, Desalination, 376 (2015) 117–129.
[27] A. Alkhudhiri, N. Darwish, N. Hilal, Treatment of saline solutions using air gap membrane distillation: experimental study, Desalination, 323 (2013) 2–7.
[28] L.D. Nghiem, F. Hildinger, F.I. Hai, T. Cath, Treatment of saline aqueous solutions using direct contact membrane distillation, Desal. Wat. Treat., 32 (2011) 234–241.
[29] A. Criscuoli, M.C. Carnevale, E. Drioli, Evaluation of energy requirements in membrane distillation, Chem. Eng. Process. Process Intensif., 47 (2008) 1098–1105.
[30] J. Sanmartino, M. Khayet, M. García-Payo, H. El Bakouri, A. Riaza, Desalination and concentration of saline aqueous solutions up to supersaturation by air gap membrane distillation and crystallization fouling, Desalination, 393 (2016) 39–51.
[31] J.A. Bush, J. Vanneste, T.Y. Cath, Membrane distillation for concentration of hypersaline brines from the Great Salt Lake: effects of scaling and fouling on performance, efficiency, and salt rejection, Sep. Purif. Technol., 170 (2016) 78–91.
[32] H.C. Duong, M. Duke, S. Gray, P. Cooper, L.D. Nghiem, Membrane scaling and prevention techniques during seawater desalination by air gap membrane distillation, Desalination, 397 (2016) 92–100.
[33] M. Gryta, Degradation of polypropylene membranes applied in membrane distillation crystallizer, Crystals, 6 (2016) 33.